ТЕХНОЛОГІЇ ОТРИМАННЯ ТА ОБРОБКИ КОНСТРУКЦІЙНИХ МАТЕРІАЛІВ

TECHNOLOGIES OF OBTAINING AND PROCESSING OF CONSTRUCTION MATERIALS

UDC 669.017:621.78:539.4:621.771.29

Ihor Vakulenko — Doctor of Technical Sciences, Professor of the Department of Condensed State Physics of the Dnipro State Technical University, Kamianske, Ukraine, *e-mail: vakulenko_ihor@ukr.net*, ORCID: 0000-0002-7353-1916

Serhii Plitchenko — Candidate of Technical Sciences, Associate Professor of the Department of Applied Mechanics and Materials Science of the Ukrainian State University of Science and Technologies, Dnipro, Ukraine, *e-mail: plit4enko@ukr.net*, ORCID: 0000-0002-0613-2544

Tatyana Kalinina — Candidate of Technical Sciences, Associate Professor, Head of the Department of Condensed State Physics of the Dnipro State Technical University, Kamianske, Ukraine, *e-mail: kalinina_tv@ukr.net*, ORCID: 0000-0002-6806-3425

EFFECT OF AUSTENITE DEGRADATION CONDITIONS ON THE PROPERTIES OF STEEL 20

Purpose. *To investigate the nature of property changes in thermally strengthened coiled steel 20 depending on the mechanism of austenite degradation.*

Research methods. *The material for study was a wire with a diameter of 3 mm, made of low-carbon steel, with 0.22 % C, 0.46 % Mn, 0.088 % Si, 0.1 % Cr, 0.03 % S, 0.012 % P. The different structure state of the steel was obtained after certain processing. The samples, 0.3 m long, were subjected to austenitization at a temperature of 920 °C for 8 min, after that for 10 min followed isotherm exposure, at temperatures of 650–200 °C and tempering at temperature of isothermal transformation, duration by 60 min. The microstructure was studied using light and electron microscopy. Dimensions of structural element were determined by quantitative metallography methods. The mechanical properties were determined from analyzing tensile curves at room temperature and strain rate of* 10^{-3} s^{-1}.

Results. *The change at structure and properties is largely determined by the mechanism of austenite transformation under isothermal conditions. During diffusion transformation of austenite, the dispersion of the phase components is accompanied by an increase at super saturation of the solid solution by carbon. For the intermediate transformation region, a change at phase composition of the steel is added. The subsequent tempering determines the kinetics and degree of completion processes of structure formation of the thermally hardened rolled steel. At low tempering temperatures of steel with a bainite structure, hardening is due to the development of aging processes. With an increase at tempering temperature, the development of softening processes is accelerated.*

Scientific novelty. *The increase plasticity of the steel with a bainite structure is due to a decrease of dispersion of cementite particles, dislocation density, and the development of polygonization at initial stages of recrystallization. The softening of steel with a ferrite-pearlite structure is determined by a decrease in phase hardening during austenite transformation.*

Practical value. *Mechanism analysis of structural transformations has determined that manufacture of thermally strengthened rolled steel, the expected softening after coiling is recommended to compensate by a corresponding decrease of temperature of the end of accelerated cooling.*

Key words: *low-carbon steel, isothermal transformation, austenite, ferrite, pearlite, dispersion.*

Introduction

In metallurgical production, the enhancement of strength and service properties of products can be achieved via two fundamentally different technological approaches. The required phase composition of steel is obtained by adjusting the concentration ratios of chemical elements [1, 2], which ultimately determines the basic structure and property set of the rolled product. At the same time, the morphology and dispersion of phase constituents are governed by the conditions of the final stage of product manufacturing [2, 3].

DOI 10.15588/1607-6885-2026-1-4

Another approach to modifying the structure and properties of metallurgical products involves targeted variation of the heating and cooling temperature-rate parameters [4, 5]. This technology can be applied both to individual products and to billets at intermediate processing stages. The variety of such processing schemes is generally referred to as thermal strengthening technology.

Compared to altering the phase composition of steel through alloying, the use of thermal treatment technologies significantly expands the possibilities for structural modification during the production of iron-carbon alloys [6, 7]. This provides an additional factor for change not only in the morphology and dispersion of phase constituents, but also in their nature and quantitative ratio during structure formation [8].

The allotropic transformation of iron and the thermokinetic conditions of cooling form the basis for obtaining a variety of phase constituents, depending on the component ratios and the degree of undercooling relative to the critical temperatures of phase equilibrium.

Analysis of research and publication

Compared to the structure of low-carbon steel after hot plastic deformation, the use of thermal strengthening in the rolling mill flow leads to qualitative changes in the structure and the corresponding set of properties [9, 10]. Proportionally to the cross-sectional thickness of the rolled product, the complexity of achieving the critical cooling rate results in the formation of a structural gradient, starting from the surface with intensive heat removal. The continuous decrease in cooling rate with increasing distance from the surface determines the structural state and the corresponding set of properties [11]. Thus, the structural gradient formed along the cross-section of the rolled product is determined by the temperature at the end of forced cooling for a given metal volume [6].

Compared to the production of metallic products in the form of rods, the manufacture of rolled products wound into a bundle has its own specific features [12, 13]. One of these is the additional thermal effect on the metal after the completion of forced cooling and coiling into a bundle [14, 15]. Indeed, after coiling, the rolled product remains for some time under the influence of the final accelerated cooling temperature. The duration of this thermal exposure at tempering is proportional to the mass of metal in the coil. Therefore, additional holding at such temperatures inevitably affects the structure and the associated set of properties of the rolled product [1, 5].

Meeting certain challenges, the additional thermal effect on the structure and properties of thermally strengthened rolled steel, which is wound into a bundle, can be evaluated by modeling the structural transformation processes in the metal. For this purpose, thermal strengthening in the rolling mill flow and holding the metal at the coiling temperature can be represented as alternating isothermal transformation at a certain temperature (below A_{c1}) and holding at this temperature.

Research material and methodology

The material selected for the study was a 3 mm diameter low-carbon steel wire with the following chemical composition: 0.22 % *C*, 0.46 % Mn, 0.088 % Si, 0.1 % Cr, 0.03 % S, and 0.012 % P.

Different structural states of the steel were obtained through specific thermal treatments. Wire samples, 0.3 m in length, were austenitized at 920 °C for 8 minutes. This was followed by isothermal holding for 10 minutes at temperatures ranging from 650 °C to 200 °C, and subsequent tempering at the isothermal transformation temperature for 60 minutes. Heating to the austenitization temperature, isothermal holding, and tempering were carried out in molten mixtures of various salts.

Sample preparation for microstructural analysis was performed in accordance with the requirements of light and electron microscopy [16]. To reveal the microstructure, specimens were etched using a standard reagent (4 % HNO_3 solution in ethanol).

Mechanical properties, including strength, ductility, and the strain hardening coefficient, were determined by analyzing tensile curves [17, 18] obtained at room temperature and a strain rate of 10^{-3} s^{-1}.

In the first stage, the technical tensile diagram was converted into a true stress-strain diagram and then plotted in logarithmic coordinates (Fig. 1).

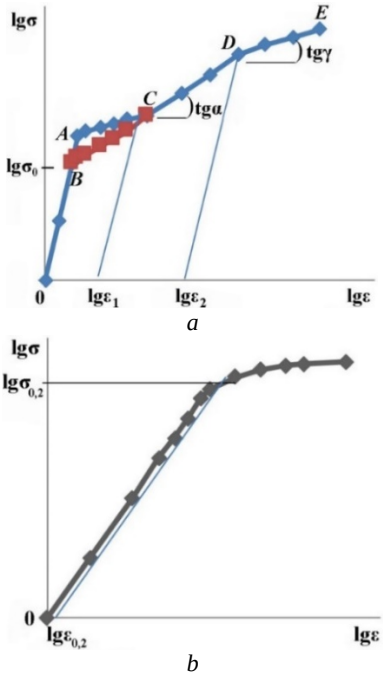

Figure 1. Schematic view of true tension diagrams in logarithmic coordinates:
a – with a section of discontinuous flow and *b* – without it

From the technical tensile curve in the coordinates "applied load (P_i) – sample elongation (Δl_i)", where elongation was calculated as $\Delta l_i = l_k - l_0$ (with l_0 and l_k being the initial and final gauge lengths, respectively), the true

DOI 10.15588/1607-6885-2026-1-4

stress (σ_i) and true strain (ε_i) were calculated. The calculation method was based on the assumption of constant of metal volume during plastic deformation.

True strain was calculated using the relation $\varepsilon_i = \ln(l_k/l_0)$.

To calculate the true stress (σ_i), it is necessary to estimate the current cross-sectional area (F_i) of the gauge section of the specimen after loading with force P_i. Considering the constancy of the metal volume in the gauge section, after elongation by Δl_i, the cross-sectional area decreases accordingly to the value F_i. Thus, the true stress is determined as: $\sigma_i = P_i/F_i$.

Based on the current values of σ_i and ε_i obtained from the true tensile curves (σ_i and ε_i), the strength characteristics were determined, including the yield strength (σ_y) and ultimate tensile strength (σ_S). The relative elongation (δ) was calculated using the relation: $\delta = [\Delta l_i/l0]\cdot 100$ %.

Further, by analyzing the constructed tensile curve in the coordinates $\lg \sigma_i - \lg \varepsilon_i$ (Fig. 1*a*), the strain hardening coefficient (n) was determined. This coefficient is the exponent in the equation $\sigma = K\cdot\varepsilon_n$, which describes the general form of the deformation curve. The value of n was determined as the tangent of the slope angle (α) in the initial segment (CD) of uniform strain hardening, according to: $tg\alpha = \Delta\lg \sigma_i/\Delta\lg \varepsilon_i$.

Results and their discussion

The process of structure formation in thermally strengthened coiled steel after the completion of hot deformation can be divided into two stages. The first stage ends when the rolled product reaches a certain temperature after accelerated cooling. The structural state at this point corresponds to the conditions of isothermal austenite transformation at the temperature of the end of accelerated cooling.

In the second stage, structural transformations occur due to the thermal effect on the metal after it is coiled. In terms of its effect on the structure and properties of the metal, the thermal influence after coiling into a bundle is equivalent to tempering at the isothermal austenite transformation temperature [8, 11].

Accepting the concept of two-stage structure formation in rolled products, it is first necessary to consider the effect of the isothermal austenite transformation temperature on the structure and properties of low-carbon steel. In the temperature range up to the minimum stability of austenite, the diffusion transformation mechanism determines the morphology and dispersion of the structural constituents of the studied steel [19, 20]. At transformation temperatures starting from 650 °C, the structure consists of a small amount of regions similar to Widmanstätten ferrite (Fig. 2*a*), polyhedral ferrite grains, and pearlite colonies of defined dispersion. It should be noted that at isothermal austenite transformation temperatures under the diffusion mechanism, structure formation is determined by the quantitative ratios and dispersion of the structural constituents, without qualitative changes in the phase composition of the steel.

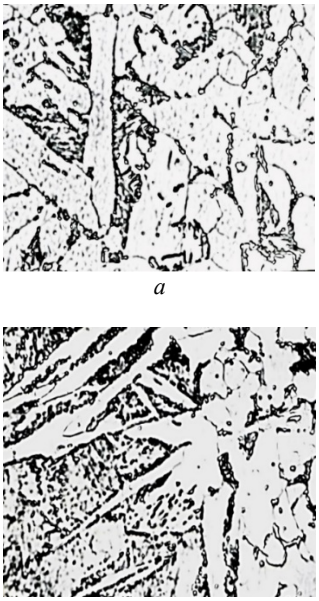

a

b

Figure 2. Microstructure of steel 20 after isothermal transformation at 650 °C (*a*) and 600 °C (*b*). Magnification: ×1000

Indeed, when the isothermal transformation temperature is reduced to 600 °C, alongside the refinement of structural constituents, a progressive decrease in the number of polyhedral ferrite grains is observed, accompanied by an increase in the fraction of Widmanstätten ferrite (Fig. 2*b*). The absence of qualitative changes in the steel structure at this transformation temperature is explained by the insufficient stability of austenite during cooling [11, 19], which is analogous to the effect of reduced carbon concentration in steel.

Further lowering the isothermal transformation temperature of austenite to the range of 500–400 °C, while structural refinement continues, leads to the emergence of initial signs of qualitative changes in the steel's phase composition (Fig. 3*a*). As the average size and volume fraction of polyhedral ferrite grains decrease, the amount of Widmanstätten ferrite increases [20], and changes in its morphology begin to appear (Fig. 3*b*).

A clear confirmation of this phenomenon is the microstructure of steel after isothermal transformation at 400 °C (Fig. 3*c*). Compared to the number of individual Widmanstätten ferrite plates formed at 500 °C (Fig. 3*a*), their quantity is significantly lower at 400 °C.

Proportional to the decrease in transformation temperature, the dispersion of compactly arranged cementite particles increases (Fig. 3*d*). Moreover, it should be noted that Widmanstätten ferrite begins to form in two distinct morphologies: as branched structures and as plate-like packets (Fig. 3*c*).

DOI 10.15588/1607-6885-2026-1-4

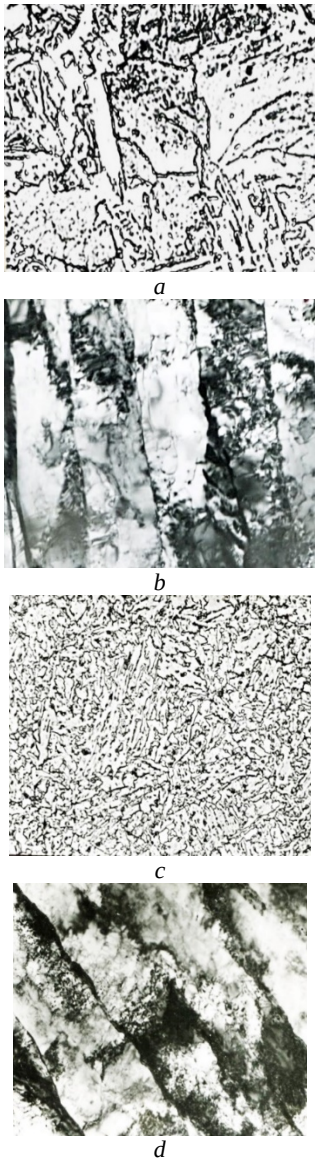

Figure 3. Microstructure of steel 20 after isothermal transformation at 500 °C (*a*, *b*) and 400 °C (*c*, *d*). Magnification: ×1000 (*a*, *c*), ×14,000 (*b*, *d*)

The observed structural changes should be considered as an approach to the temperature range where a change in the austenite transformation mechanism may occur [15, 19]. Based on this, when the isothermal transformation temperature drops below 400 °C, qualitative changes in the structural state of the steel are expected.

The microstructure formed after isothermal transformation at 300 °C and 200 °C confirms these expectations. Considering that even a slight decrease in the transformation temperature starting from 350 °C leads to a rapid reduction in the number of polyhedral ferrite grains [12, 20], their presence at 300 °C becomes difficult to detect (Fig. 4*a*, *b*).

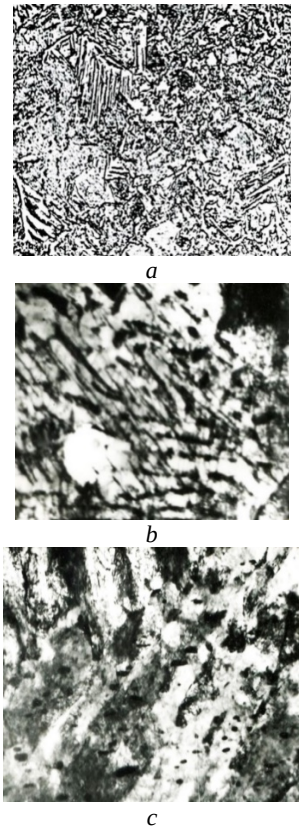

Figure 4. Microstructure of steel 20 after isothermal transformation at 300 °C. Magnification: ×1000 (*a*), ×18,000 (*b*, *c*)

Simultaneously, regions resembling highly dispersed pearlite colonies begin to appear (Fig. 4*b*), and the emergence of metal volumes with a bainite-like structure (Fig. 4*c*) should be considered as confirmation of the onset of qualitative changes. After lowering the isothermal transformation temperature to 200 °C, it becomes extremely difficult to identify any signs of austenite transformation via the shear mechanism based on the steel's microstructure (Fig. 5).

The microstructure mainly consists of bainitic crystals (Fig. 5*a*, *b*) and a number of finely dispersed cementite particles with localized distribution (Fig. 5*c*). One of the reasons for the absence of martensite is the low stability of austenite in low-carbon steel due to the high temperature of onset of martensitic transformation (M_S). The M_S temperature can be estimated using the following relation:

$$M_S = 520 - 320(\%\ C) - 50(\%\ Mn) - 30(\%\ Cr) - 20(\%\ Ni + \%\ Mo) - 5(\%\ Si + \%\ Cu). \quad (1)$$

where % *C* is concentration of the carbon and other chemical elements.

Using equation (1), the calculated martensite start temperature for the investigated steel is 423 °C, which corresponds well with known experimental data (420–400 °C) [12, 19]. Based on this, preventing intermediate decomposition of austenite during cooling and isothermal holding at 200 °C is a rather challenging task.

DOI 10.15588/1607-6885-2026-1-4

As a result of partial austenite decomposition, proportional to the degree of undercooling starting from temperatures around 400 °C, there is a gradual increase in the volume fraction of the bainitic component in the steel structure.

Overall, it can be considered that during isothermal holding of low-carbon steel at temperatures close to M_S, qualitatively similar structures are formed, differing only in the ratio of structural constituents and their dispersion [6, 11].

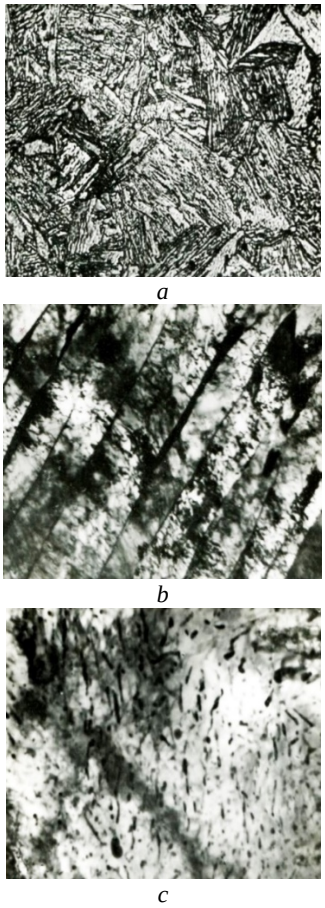

a

b

c

Figure 5. Microstructure of steel 20 after isothermal transformation at 200 °C. Magnification: ×1000 (*a*), ×18,000 (*b*, *c*)

When the temperature drops below M_S, the products of austenite transformation by the diffusion mechanism are gradually replaced by those formed via the intermediate mechanism [9]. The transformation of the steel structure depending on the isothermal austenite transformation temperature is accompanied by corresponding changes in mechanical properties (Fig. 6).

In view of the fact that range changes in the relative narrowing is 73–75 %, uniform elongation (δ_P) was used as a characteristic plasticity of the steel.

Analysis of presented dependencies shows that increasing the isothermal transformation temperature is accompanied by a predictable decrease in strength characteristics (Fig. 6*a*, *b*) and an increase in ductility (Fig. 6*c*). At the same time, the metal's ability for strain hardening changes according to a more complex relationship (Fig. 6*d*).

Overall, the non-monotonic nature of the changes in steel properties indicates the need to conventionally divide the temperature axis of the curves into separate regions: *I* (650–500 °C), *II* (450–350 °C), and *III* (300–200 °C).

For region *I* (Fig. 6), starting from 650 °C, the gradual decrease in the isothermal transformation temperature down to 500–450 °C is accompanied by a monotonic decrease in elongation (δ_P), an increase in strength characteristics (yield strength σ_y and ultimate tensile strength σ_S), and an increase in the metal's strain hardening ability (n).

This behavior of mechanical properties is explained by the evolution of the structure and changes in the phase composition of the steel. According to microstructural analysis, when the isothermal transformation temperature decreases from 650–600 °C (Fig. 2) to 500 °C (Fig. 3*a*, *b*), there are practically no qualitative changes in the structural state.

The phase composition remains constant, with only the quantitative ratio and dispersion of the structural constituents changing. In general, the increase in strength properties is due to the growth in the amount of Widmanstätten ferrite, the reduction in the size of polyhedral ferrite grains (d_P), and the thickness of the ferrite interlamellar spacing in pearlite colonies (λ) [2, 19].

According to stoichiometry for the investigated steel under nearly equilibrium conditions, the amount of pearlite does not exceed 30 %, for temperatures of 650–600 °C, d_P can be considered the main structural element.

At the same time, the presence of Widmanstätten ferrite may, to some extent, distort the influence of d_P on the overall properties of the steel.

Indeed, the well-known effect of ferrite grain size on strength characteristics will be observed only in the absence of excessive supersaturation of ferrite with carbon atoms and in the presence of substructural features.

When d_P serves as the main structural element for low-carbon steel, the strain hardening coefficient and plasticity of steel are directly proportional [22].

For pearlite colonies, a qualitatively different relationship is observed: a decrease in λ leads to a decrease in n, which promotes an increase in the ductility of eutectoid steel. Thus, as the transformation temperature decreases from 650 to 500 °C, the reduction in d_P, along with an increase in the amount of Widmanstätten ferrite and a higher degree of ferrite supersaturation with carbon atoms, contributes to a decrease in elongation (δ_P). Considering that the dispersion of pearlite colonies should increase δ_P, the amount of pearlite is insufficient to compensate for the effect of d_P, resulting in an overall decrease in δ_P. At the same time, the strain hardening coefficient and d_P are inversely proportional (Fig. 6*c*, *d*).

DOI 10.15588/1607-6885-2026-1-4

A further decrease in the isothermal austenite transformation temperature in region *II* is accompanied, similarly to region *I*, by an increase in strength and a decrease in relative elongation. The exception is the behavior of the strain hardening coefficient *n*.

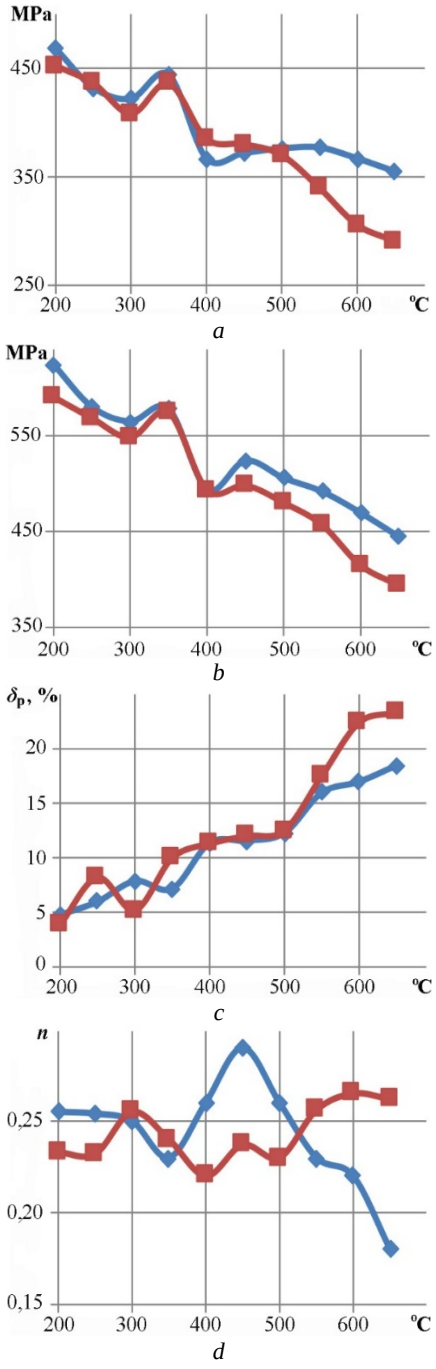

Figure 6. Variation of yield strength (*a*), ultimate tensile strength (*b*), uniform elongation (δ_P) (*c*), and strain hardening coefficient (*n*) (*d*) depending on the isothermal transformation temperature (♦) and subsequent tempering at this temperature (■)

The nature of the dependence of *n* indicates the emergence of structural changes in the steel that can influence the development of strain hardening processes (Fig. 6*d*). Indeed, microstructural analysis (Fig. 3*c*) shows that lowering the isothermal transformation temperature from 450–400 °C is accompanied by an increase in the amount of Widmanstätten ferrite due to a decrease in the number of polyhedral ferrite grains. Simultaneously, there is an increase in regions containing locally distributed dispersed cementite particles, similar to remnants of pearlite colonies. Moreover, according to studies [19, 20] of steels with similar composition, after isothermal austenite transformation at 450–400 °C, the structure is expected to contain areas resembling bainitic crystals. Thus, the appearance of the bainitic phase should be considered one of the reasons for qualitative changes in the property dependencies of the steel.

Against the background of a sharp decrease in the strain hardening coefficient in the temperature range of 450–400 °C, the ability of the bainitic phase to undergo plastic deformation [11] should be regarded as one of the reasons for the change in the rate of decrease of elongation δ_P. On the other hand, at 350 °C, the almost complete disappearance of Widmanstätten ferrite and the increase in the amount of bainitic phase, together with the refinement of cementite particles and a decrease in the amount of pearlite colonies (Fig. 4*a*, *b*), collectively lead to a sharp reduction in the ductility of the steel.

As an additional source of δ_P reduction, the differences in the strain hardening ability of bainite and pearlite should be considered, as confirmed by the relationship between n and δ_P (Fig. 6*d*, designation ♦).

Region *III*. Lowering the temperature from 300 to 200 °C results in the formation of a bainitic structure (Fig. 4, 5). This promotes an increase in the strain hardening effect, which is primarily due to the supersaturation of the solid solution with carbon atoms during bainite formation [2, 11] and dispersion strengthening from carbide phase particles (Fig. 4*b*, *c*) [20, 21].

Compared to isothermal transformation, the additional effect of tempering has a distinct impact on the nature of property changes in the steel (Fig. 6). In general, the difference in the dependence of mechanical properties on tempering temperature is reasonably consistent with the formed structural state of the metal. On the other hand, it should be noted that the tempering temperature has a different effect on the change of specific properties. This is due to the dependence of steel properties on the development of strain hardening processes.

Thus, for the temperature range from 200 to 500 °C, significant differences in the values of σ_y and δ_P are observed at a tempering temperature of about 500 °C (Fig. 7*a*, *c*), while for σ_S and the strain hardening coefficient (Fig. 7*d*), the temperature is lower and is approximately 400 °C (Fig. 7*b*).

DOI 10.15588/1607-6885-2026-1-4

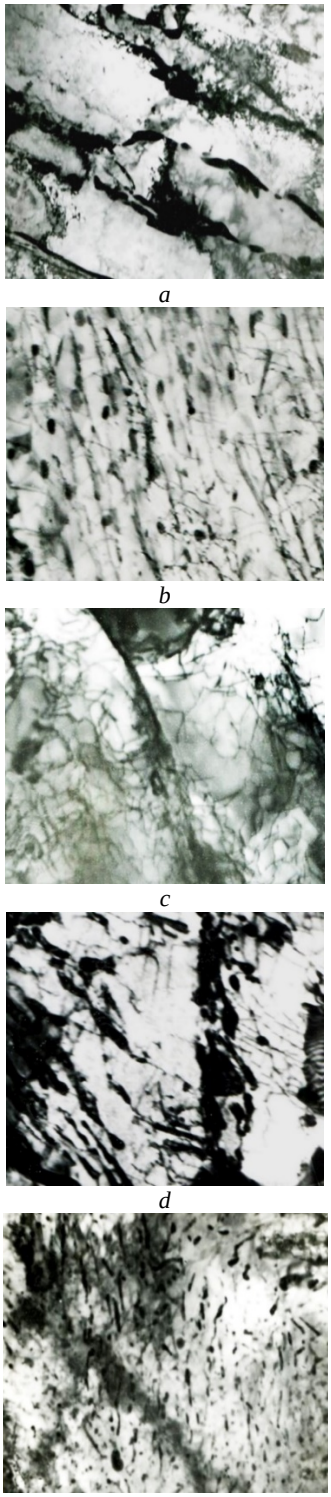

Figure 7. Microstructure of steel 20 after isothermal transformation at 500 °C and tempering at the same temperature (*a*, *b*); at 600 °C (*c*, *d*); and at 650 °C (*e*). Magnification: ×6000 (*a*), ×10,000 ×1.5 (*b*–*e*)

Compared to yield strength (σ_y), the lower tempering temperature at which differences in ultimate tensile strength (σ_S) appear is attributed to the development of strain hardening processes. Considering that in the region of initial plastic deformation (at the level of σ_y), the contribution of strain hardening is minimal [22], while at the level of σ_S, its influence becomes significant. The nature of the dependence of the strain hardening coefficient (n) on tempering temperature (Fig. 7*d*) confirms this reasoning. Based on this, it can be concluded that minor structural changes during tempering, to which σ_y is insensitive, will affect σ_S due to the development of strain hardening.

Compared to strength properties, the strain hardening coefficient is a more sensitive indicator of structural changes, both after isothermal transformation and subsequent tempering. Indeed, qualitative changes in the phase composition of steel due to isothermal transformation temperature correspond to changes in the nature of the n-dependence, with clear segmentation between regions (Fig. 6*d*).

After the temperature range of 200–300 °C lies the region of 350–450 °C (Fig. 6*d*), which corresponds to the transition from substructural strengthening to the emergence of strengthening due to the presence of ferrite grain boundaries [16, 17]. Thus, the nearly identical behavior of property changes up to 450–500 °C indicates the absence of qualitative differences in the metal's structure. Compared to isothermal transformation at 500 °C (Fig. 3*b*, *d*), additional tempering at this temperature leads to dislocation redistribution within Widmanstätten ferrite regions (Fig. 7*a*). These changes visually correspond to the development of polygonization processes. As a result of subboundary formation, ferrite grains are subdivided into microvolumes and partially cleared of unconnected dislocations (Fig. 7*a*). At the same time, dispersed particles that are excretion at sub-boundaries contribute to the development of dispersion strengthening.

Dislocation redistribution is inevitably accompanied by their annihilation, reducing the accumulated dislocation density resulting from phase hardening after isothermal austenite transformation.

Similar structural changes are observed in ferrite microvolumes with compactly arranged cementite particles (Fig. 7*b*). Dislocations blocked at cementite particles form a sub-boundary-like network. However, the extent of structural evolution during tempering is insufficient to fully explain the nature of property changes. The relatively small softening effect after tempering at 500 °C (Fig. 6) should be considered as the result of competing structural transformation processes. The softening effect from polygonization is partially offset by dispersion strengthening from cementite particles precipitated along sub-boundaries during tempering.

As the tempering temperature increases, the acceleration of diffusion-driven mass transfer enhances the softening effect. The initial stages of dislocation redistribution at 500 °C are further intensified at 550–600 °C (Fig. 7*c*, *d*).

In addition to polygonization, tempering at 600 °C is accompanied by the onset of recrystallization processes in regions of Widmanstätten ferrite (Fig. 7*c*).

DOI 10.15588/1607-6885-2026-1-4

Visually, this is manifested as a change in the development of recrystallization mechanism – from the migration of high-angle grain boundaries to the disappearance of low-angle boundaries, similar to those separating adjacent plates of Widmanstätten ferrite (Fig. 7*c*) [11, 16]. This recrystallization mechanism is typical for alloys with structures formed through the presence of boundaries with misorientation angles in the range of 1.5–2°.

Due to the low energy of such boundaries, no additional energy is required for their migration during recrystallization; instead, neighboring subgrains merge through the elimination of the boundary between them [16]. The growth of subgrains, via a mechanism similar to coalescence, is partially hindered by the presence of dispersed cementite particles (Fig. 7*d*), which also act as obstacles to dislocation annihilation [23].

Overall, recrystallization in Widmanstätten ferrite regions leads to the formation of polyhedral ferrite grains, similar to those shown in Fig. 2*a*.

Moreover, considering the interdependence of the process's ferrite recrystallization, spheroidization and cementite coalescence processes, the localized distribution of cementite particles contributes to the refinement of ferrite grains.

As a result, tempering at 600 °C leads to the formation of a highly heterogeneous ferrite structure (Fig. 7*d*). Similar structural changes are observed in steel tempered at 650 °C (Fig. 7*e*).

Compared to the structure after isothermal austenite transformation, where the strain hardening coefficient (n) and elongation (δ_P) are mostly inversely related (Fig. 8), additional tempering starting from 500 °C results in a direct proportional relationship between these characteristics (Fig. 6*c*, *d* and 8).

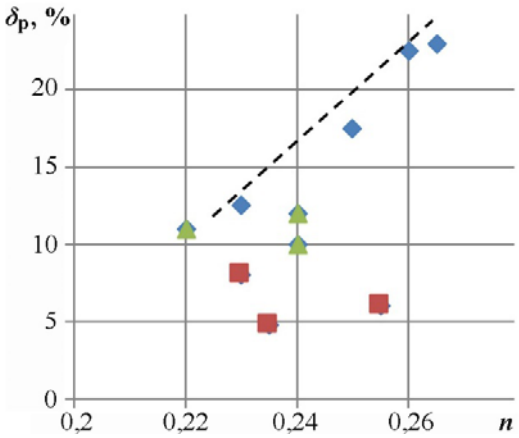

Figure 8. Correlation between elongation (δ_P) and strain hardening coefficient (n) after isothermal transformation and tempering within the temperature ranges: 500–650 °C (♦); 350–450 °C (▲); 200–300 °C (■)

The validity of this correlation is confirmed by the increase in ductility of low-carbon steel during cold rolling, which is proportional to the ferrite grain size. In fact, the observed relationship is based on the enhanced ability of low-carbon steels to undergo strain hardening, which increases proportionally with ferrite grain size [22].

Detailed analysis of substructural changes in deformed low-carbon steel has shown that the direct correlation between ferrite grain size (d_P), strain hardening coefficient (n), and elongation (δ_P) is rooted in the ability of the dislocation cell structure to evolve. The larger the ferrite grain size, the earlier the breakdown of uniform dislocation distribution into periodic structures begins, even at lower accumulated dislocation densities [16, 17].

Considering that the size of a dislocation cell is proportional to the ferrite grain size, the larger the d_P, the smaller the difference in dislocation concentration between the cell boundary and its interior.

As a result, the larger the dislocation cell and the lower the total dislocation density, the greater the cell's ability to evolve during metal deformation. Therefore, in low-carbon steel, the capacity for dislocation accumulation until reaching the maximum allowable concentration increases proportionally with ferrite grain size. Consequently, the increase in ductility of low-carbon steel with increasing ferrite grain size is fully justified. In this context, the strain hardening coefficient in low-carbon steel subjected to significant plastic deformation is often used as a controlling parameter.

Conclusions

The influence of the isothermal transformation temperature on the balance between strength and ductility of steel characteristics of low-carbon rolled products is determined by the mechanism of austenite degradation and the duration of holding after coiling into a bundle. Based on the analysis of the research results, it was found that the increase in ductility of steel during austenite transformation via the intermediate mechanism is achieved through the growth of cementite particle size, reduction in dislocation density due to polygonization, and the onset of recrystallization. For steel with ferrite-pearlite structures, ductility is proportional to the reduction in phase hardening effects and the degree of ferrite supersaturation with carbon atoms.

From a technological standpoint, the softening effect of coiled into a bundle thermally strengthened steel is proposed to be compensated by appropriately lowering the final temperature of forced cooling. This temperature should be determined based on the level of metal strengthening and the coil mass.

References

1. Liu, M., Wang, J., Zhang, Q., Hu, H., & Xu, G. (2021). Optimized properties of a quenching and partitioning steel by quenching at fine martensite start temperature. Metals and Materials International, 27, 2473–2480. https://doi.org/10.1007/s12540-020-00726-5.

DOI 10.15588/1607-6885-2026-1-4

2. Deineko, L. M., Borysenko, A. Yu., Taranenko, A. A., Zaitseva, T. O., & Romanova, N. S. (2021). Features of the ferrite-bainite structure low-alloy low-carbon steel after heat hardening and subsequent tempering. Metal Science and Heat Treatment of Metals, 2(93), 33–47. https://doi.org/10.30838/J.PMHTM.2413.270421.33.739

3. Liu, J.-H., Binot, N., Delagnes, D., & Jahazi, M. (2021). Influence of the cooling rate below Ms on the martensitic transformation in a low alloy medium-carbon steel. Journal of Materials Research and Technology, 12, 234–242. https://doi.org/10.1016/j.jmrt.2021.02.075

4. Morawiec, M., Skowronek, A., Król, M., & Grajcar, A. (2020). Dilatometric analysis of the austenite decomposition in undeformed and deformed low-carbon structural steel. Materials, 13(23), 5443. https://doi.org/10.3390/ma13235443

5. Bharadwaj, R., Sarkar, A., & Rakshe, B. (2022). Effect of cooling rate on phase transformation kinetics and microstructure of Nb–Ti microalloyed low carbon HSLA steel. Metallography, Microstructure, and Analysis, 11, 661-672. https://doi.org/10.1007/s13632-022-00864-9

6. Beketov, O. V., Laukhin, D. V., Osypchuk, M. M., Pomazan, A. R., & Radko, O. V. (2025). Study of the influence of accelerated cooling on the kinetics of destruction of low-carbon low-alloy steels. Ukrainian Journal of Civil Engineering and Architecture, (1)025, 17–24. https://doi.org/10.30838/UJCEA.2312.270225.17.1124

7. Mondal, J., Das, K., & Das, S. (2021). Isothermal transformation kinetics, microstructure and mechanical properties of a carbide free bainitic steel. Materials Characterization, 177, 111166. https://doi.org/10.1016/j.matchar.2021.111166

8. Zhang, J., Gu, S., Wang, J., Wei, F., Li, Z., Zeng, Z., Shen, B., & Li, C. (2024). Effect of isothermal transformation temperature on the microstructure, precipitation behavior, and mechanical properties of anti-seismic rebar. High Temperature Materials and Processes, 43(1), 20240028. https://doi.org/10.1515/htmp-2024-0028

9. Li, J., Yang, Z., Ma, H., Chen, C., & Zhang, F. (2023). A medium-C martensite steel with 2.6 GPa tensile strength and large ductility. Scripta Materialia, 228, Article 115327. https://doi.org/10.1016/j.scriptamat.2023.115327

10. Singh, P. P., Ghosh, S., & Mula, S. (2022). Strengthening behaviour and failure analysis of hot-rolled Nb+V microalloyed steel processed at various coiling temperatures. Materials Science and Engineering: A, 859, 144210. https://doi.org/10.1016/j.msea.2022.144210

11. Vakulenko, I., Plitchenko, S., Gubarev, S., & Khlebnikov, A. (2024). Structural changes during thermal strengthening of the railway wheel. New Materials and Technologies in Metallurgy and Mechanical Engineering, 2, 6-12. https://doi.org/10.15588/1607-6885-2024-2-11

12. Gu, C., Scott, C., Fazeli, F., Gaudet, M. J., Su, J., Wang, X., Bassim, N., & Zurob, H. (2023). Evolution of the microstructure and mechanical properties of a V-containing microalloyed steel during coiling. Materials Science and Engineering: A, 880, 145332. https://doi.org/10.1016/j.msea.2023.145332

13. Dai, M., Hu, Y., Hao, Y., Qiu, P., & Xiao, H. (2025). Analysis of temperature and stress fields in the process of hot-rolled strip coiling. Metals, 15(2), 111. https://doi.org/10.3390/met15020111

14. Dai, M., Liang, S., Qiu, P., & Xiao, H. (2024). Efficient finite element simulation of cold rolled strip coiling process considering additional contact deformation between layers. ISIJ International, 64, 1037-1046. https://doi.org/10.2355/isijinternational.ISIJINT-2023-405

15. Wang, C., Wu, H., & Zhang, Y. (2024). Structural transformation behavior of oxide scale during coiling of 0.9wt% Cr-containing high-strength steel. Journal of Materials Research and Technology, 30, 840–853. https://doi.org/10.1016/j.jmrt.2024.03.094

16. Sukhomlin, G. (2013). Special boundaries in ferrite of low-carbon steels. Metallophysics and Advanced Technologies, 35(9), 1237-1249 [in Russian]. Retrieved from http://dspace.nbuv.gov.ua/bitstream/handle/123456789/104215/11-Sukhomlin.pdf?sequence=1

17. Vakulenko, I.O., Vakulenko, L.I., Bolotova, D.M., Kurt, B., Asgarov, H., & Colova, O. (2022). Influence structure on the plasticity of carbon steel of the railway wheel rim in operation. Scientific Journal of Silesian University of Technology, Series Transport, 115, 183-192. http://dx.doi.org/10.20858/sjsutst.2022.115.13

18. Tsuchida, N., Inoue, T., & Nakado, H. (2013). Effect of ferrite grain size on the estimated true stress –strain relationship up to the plastic deformation limit in low carbon ferrite – cementite steels. Journal of Materials Research, 28(18), 2171–2179. https://doi.org/10.1557/jmr.2013.221

19. Vakulenko, I., Plitchenko, S., Bolotova, D., & Asgarov, Kh. (2023). Influence hot plastic deformation on the structure and properties of carbon steel of the railway wheel. Scientific Journal of Silesian University of Technology, Series Transport, 121, 257–266. https://doi.org/10.20858/sjsutst.2023.121.16

20. Zhao, S., Min, N., & Li, W. (2022). Formation of Widmanstätten ferrite and grain boundary ferrite in a hypereutectoid pearlitic steel. Metals, 12(3), 493. https://doi.org/10.3390/met12030493

21. Liu, G., Li, Y., Liao, T., Wang, S., Lv, B., Guo, H., Huang, Y., Yong, Q., & Mao, X. (2023). Revealing the precipitation kinetics and strengthening mechanisms of a 450 MPa grade Nb-bearing HSLA steel. Materials Science and Engineering: A, 884, Article 145506. https://doi.org/10.1016/j.msea.2023.145506

22. Vakulenko, I. A., Plitchenko, S., & Yılmaz, A. F. (2025). Influence degree and scheme of hot reduction on properties of the carbon steel. Manufacturing Technologies and Applications, 6(1), 150–156. https://doi.org/10.52795/mateca.1634663.

DOI 10.15588/1607-6885-2026-1-4

23. Wang, J., Hong, H., Huang, A., Yang, X., Qian, R., & Shang, C. (2022). New insight into the relationship between grain boundaries and hardness in bainitic/martensitic steels from the crystallographic perspective. Materials Letters, 308, 131105. https://doi.org/10.1016/j.matlet.2021.131105

Received 02.02.2026
Accepted 17.02.2026
Published 31.03.2026

ВПЛИВ УМОВ ДЕГРАДАЦІЇ АУСТЕНІТУ НА ВЛАСТИВОСТІ СТАЛІ 20

Ігор Вакуленко — д-р техн. наук, професор, професор кафедри фізики конденсованого стану Дніпровського державного технічного університету, м. Кам'янське, Україна, *e-mail: vakulenko_ihor@ukr.net,* ORCID: 0000-0002-7353-1916

Сергій Плітченко — канд. техн. наук, доцент, доцент кафедри прикладної механіки та матеріалознавства Українського державного університету науки і технологій, м. Дніпро, Україна, *e-mail: plit4enko@ukr.net,* ORCID: 0000-0002-0613-2544

Тетяна Калініна — канд. техн. наук, доцент, завідувач кафедри фізики конденсованого стану Дніпровського державного технічного університету, м. Кам'янське, Україна, *e-mail: kalinina_tv@ukr.net,* ORCID: 0000-0002-6806-3425

Мета роботи. *Досліджено характер зміни властивостей термічно зміцненого бунтового прокату зі сталі 20 залежно від механізму деградації аустеніту.*

Методи дослідження. *Матеріалом для дослідження обраний дріт діаметром 3 мм з низьковуглецевої сталі, з 0,22 % C, 0,46 % Mn, 0,088 % Si, 0,1 % Cr, 0,03 % S, 0,012 % P. Різний структурний стан сталі отримували після певної обробки. Зразки довжиною 0,3 м піддавали аустенітизації при температурі 920 °C протягом 8 хв, ізотермічно витримували 10 хв, при температурах 650 – 200 °C та піддавали відпуску при температурі ізотермічного перетворення тривалістю 60 хв. Мікроструктуру досліджували з використанням світлової і електронної мікроскопії на просвіт. Розміри структурного елемента визначали за методиками кількісної металографії. Механічні властивості визначали за аналізом кривих розтягу за кімнатної температури та швидкості деформації 10^{-3} $с^{-1}$.*

Отримані результати. *Зміна структури і властивостей в більший мірі визначаються механізмом перетворення аустеніту за ізотермічних умов. За дифузійного перетворення аустеніту, диспергування фазових складових супроводжується зростанням пересичення твердого розчину на вуглець. Для області проміжного перетворення додається ще зміна фазового складу сталі. Наступний відпуск визначає кінетику та ступінь завершення процесів структуроутворення термічно зміцненого бунтового прокату. За низьких температур відпуску сталі зі структурою бейніту, зміцнення обумовлено розвитком процесів старіння. За підвищення температури відпуску прискорюється розвиток процесів пом'якшення.*

Наукова новизна. *Збільшення пластичності сталі з бейнітною структурою обумовлене зниженням дисперсності частинок цементиту, щільності дислокацій, розвитком полігонізації та початкових стадій рекристалізації. Пом'якшення сталі з ферито-перлітною структурою визначається зменшенням фазового наклепу при перетворенні аустеніту.*

Практична цінність. *За аналізом механізму структурних перетворень визначено, що при виготовленні термічно зміцненого прокату, очікуване пом'якшення після змотки в бунт можливо компенсувати відповідним зниженням температури кінця прискореного охолодження.*

Ключові слова: *низьковуглецева сталь, ізотермічне перетворення, аустеніт, ферит, перліт, дисперсність.*

Список літератури

1. Optimized properties of a quenching and partitioning steel by quenching at fine martensite start temperature [Text] / M. Liu, J. Wang, Q. Zhang, H. Hu, G. Xu // Metals and Materials International. – 2021. – Vol. 27. – P. 2473–2480. https://doi.org/10.1007/s12540-020-00726-5.

2. Features of the ferrite-bainite structure low-alloy low-carbon steel after heat hardening and subsequent tempering [Text] / L. M. Deineko, A. Yu. Borysenko, A. A. Taranenko, T. O. Zaitseva, N. S. Romanova // Metal Science and Heat Treatment of Metals. – 2021. – No. 2 (93). – P. 33–47. https://doi.org/10.30838/J.PMHTM.2413.270421.33.739

3. Influence of the cooling rate below Ms on the martensitic transformation in a low alloy medium-carbon steel [Text] / J.-H. Liu, N. Binot, D. Delagnes, M. Jahazi // Journal of Materials Research and Technology. – 2021. – Vol. 12. – P. 234–242. https://doi.org/10.1016/j.jmrt.2021.02.075

4. Dilatometric analysis of the austenite

DOI 10.15588/1607-6885-2026-1-4

decomposition in undeformed and deformed low-carbon structural steel [Text] / M. Morawiec, A. Skowronek, M. Król, A. Grajcar // Materials. – 2020. – Vol. 13, No. 23. – Art. 5443. https://doi.org/10.3390/ma13235443

5. Bharadwaj, R. Effect of cooling rate on phase transformation kinetics and microstructure of Nb–Ti microalloyed low carbon HSLA steel [Text] / R. Bharadwaj, A. Sarkar, B. Rakshe // Metallography, Microstructure, and Analysis. – 2022. – Vol. 11. – P. 661–672. https://doi.org/10.1007/s13632-022-00864-9

6. Study of the influence of accelerated cooling on the kinetics of destruction of low-carbon low-alloy steels [Text] / O. V. Beketov, D. V. Laukhin, M. M. Osypchuk, A. R. Pomazan, O. V. Radko // Ukrainian Journal of Civil Engineering and Architecture. – 2025. – No. 1. – P. 17–24. https://doi.org/10.30838/UJCEA.2312.270225.17.1124

7. Mondal, J. Isothermal transformation kinetics, microstructure and mechanical properties of a carbide free bainitic steel [Text] / J. Mondal, K. Das, S. Das // Materials Characterization. – 2021. – Vol. 177. – Art. 111166. https://doi.org/10.1016/j.matchar.2021.111166

8. Effect of isothermal transformation temperature on the microstructure, precipitation behavior, and mechanical properties of anti-seismic rebar [Text] / J. Zhang, S. Gu, J. Wang, F. Wei, Z. Li, Z. Zeng, B. Shen, C. Li // High Temperature Materials and Processes. – 2024. – Vol. 43, No. 1. – Art. 20240028. https://doi.org/10.1515/htmp-2024-0028

9. A medium-C martensite steel with 2.6 GPa tensile strength and large ductility [Text] / J. Li, Z. Yang, H. Ma, C. Chen, F. Zhang // Scripta Materialia. – 2023. – Vol. 228. – Art. 115327. https://doi.org/10.1016/j.scriptamat.2023.115327

10. Singh, P. P. Strengthening behaviour and failure analysis of hot-rolled Nb+V microalloyed steel processed at various coiling temperatures [Text] / P. P. Singh, S. Ghosh, S. Mula // Materials Science and Engineering: A. – 2022. – Vol. 859. – Art. 144210. https://doi.org/10.1016/j.msea.2022.144210

11. Structural changes during thermal strengthening of the railway wheel [Text] / I. Vakulenko, S. Plitchenko, S. Gubarev, A. Khlebnikov // New Materials and Technologies in Metallurgy and Mechanical Engineering. – 2024. – No. 2. – P. 6–12. https://doi.org/10.15588/1607-6885-2024-2-11

12. Evolution of the microstructure and mechanical properties of a V-containing microalloyed steel during coiling [Text] / C. Gu, C. Scott, F. Fazeli, M. J. Gaudet, J. Su, X. Wang, N. Bassim, H. Zurob // Materials Science and Engineering: A. – 2023. – Vol. 880. – Art. 145332. https://doi.org/10.1016/j.msea.2023.145332

13. Analysis of temperature and stress fields in the process of hot-rolled strip coiling [Text] / M. Dai, Y. Hu, Y. Hao, P. Qiu, H. Xiao // Metals. – 2025. – Vol. 15, No. 2. – Art. 111. https://doi.org/10.3390/met15020111

14. Efficient finite element simulation of cold rolled strip coiling process considering additional contact deformation between layers [Text] / M. Dai, S. Liang, P. Qiu, H. Xiao // ISIJ International. – 2024. – Vol. 64. – P. 1037–1046. https://doi.org/10.2355/isijinternational.ISIJINT-2023-405

15. Wang, C. Structural transformation behavior of oxide scale during coiling of 0.9wt% Cr-containing high-strength steel [Text] / C. Wang, H. Wu, Y. Zhang // Journal of Materials Research and Technology. – 2024. – Vol. 30. – P. 840–853. https://doi.org/10.1016/j.jmrt.2024.03.094

16. Сухомлин Г. Д. Специальные границы в феррите низкоуглеродистых сталей [Текст] / Г. Д. Сухомлин // Металлофизика и новейшие технологии. – 2013. – Т. 35, № 9. – С. 1237–1249. Режим доступа: http://dspace.nbuv.gov.ua/bitstream/handle/123456789/104215/11-Sukhomlin.pdf?sequence=1

17. Influence structure on the plasticity of carbon steel of the railway wheel rim in operation [Text] / I. O. Vakulenko, L. I. Vakulenko, D. M. Bolotova, B. Kurt, H. Asgarov, O. Colova // Scientific Journal of Silesian University of Technology, Series Transport. – 2022. – Vol. 115. – P. 183–192. http://dx.doi.org/10.20858/sjsutst.2022.115.13

18. Tsuchida, N. Effect of ferrite grain size on the estimated true stress –strain relationship up to the plastic deformation limit in low carbon ferrite – cementite steels [Text] / N. Tsuchida, T. Inoue, H. Nakado // Journal of Materials Research. – 2013. – Vol. 28, No. 18. – P. 2171–2179. https://doi.org/10.1557/jmr.2013.221

19. Influence hot plastic deformation on the structure and properties of carbon steel of the railway wheel [Text] / I. Vakulenko, S. Plitchenko, D. Bolotova, Kh. Asgarov // Scientific Journal of Silesian University of Technology, Series Transport. – 2023. – Vol. 121. – P. 257–266. https://doi.org/10.20858/sjsutst.2023.121.16

20. Zhao, S. Formation of Widmanstätten ferrite and grain boundary ferrite in a hypereutectoid pearlitic steel [Text] / S. Zhao, N. Min, W. Li // Metals. – 2022. – Vol. 12, No. 3. – Art. 493. https://doi.org/10.3390/met12030493

21. Revealing the precipitation kinetics and strengthening mechanisms of a 450 MPa grade Nb-bearing HSLA steel [Text] / G. Liu, Y. Li, T. Liao, S. Wang, B. Lv, H. Guo, Y. Huang, Q. Yong, X. Mao // Materials Science and Engineering: A. – 2023. – Vol. 884. – Art. 145506. https://doi.org/10.1016/j.msea.2023.145506

22. Vakulenko, I. A. Influence degree and scheme of hot reduction on properties of the carbon steel [Text] / I. A. Vakulenko, S. Plitchenko, A. F. Yılmaz // Manufacturing Technologies and Applications. – 2025. – Vol. 6, No. 1. – P. 150–156. https://doi.org/10.52795/mateca.1634663.

23. New insight into the relationship between grain boundaries and hardness in bainitic/martensitic steels from the crystallographic perspective [Text] / J. Wang, H. Hong, A. Huang, X. Yang, R. Qian, C. Shang // Materials Letters. – 2022. – Vol. 308. – Art. 131105. https://doi.org/10.1016/j.matlet.2021.131105

DOI 10.15588/1607-6885-2026-1-4